Scheme III

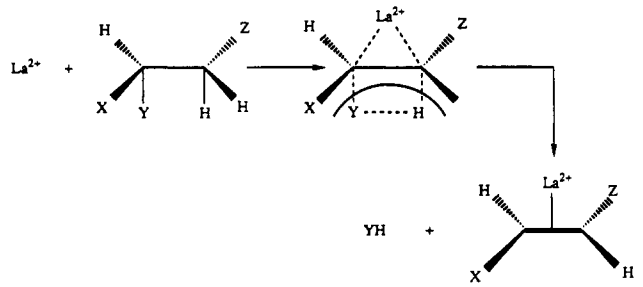

		Propane	Butane
X = CH_3 and Y = H	loss of H_2	Z = H	Z = CH_3
X = H and Y = CH_3	loss of CH_4	Z = H	Z = CH_3
X = H and Y = C_2H_5	loss of C_2H_6		Z = H

Conclusions

This study adds to the increasing amount of evidence[14] that for group 3 metal ions, the extra valence electron of the singly-charged metal ion can result in stronger bonds being formed to unsaturated hydrocarbons than for the doubly-charged species, which bind electrostatically to these ligands. Theoretical studies confirm these results and provide additional details as to the exact nature of the bonding.[20,26] Currently, the only other system that we are aware of for which there are both experimental and theoretical studies is $NbCH_2^{n+}$ (n = 1 and 2). Interestingly in this case $D°(Nb^{2+}-CH_2) > D°(Nb^{+}-CH_2)$.[27]

While La^{2+} forms primarily electrostatic bonds to hydrocarbons, its single valence electron results in the formation of strong σ bonds to radicals. This characteristic is manifested in the photodissociation of $LaC_nH_{2n}^{2+}$ (n = 2, 3) species where, in contrast to $LaC_nH_{2n}^{+}$, loss of H and CH_3 were observed, yielding strong σ-bonded complexes with the remaining ligand.

The chemistries of La^+ and La^{2+} with simple alkanes are similar, with elimination of H_2 and small alkanes observed for both, although different mechanisms are clearly involved. One exception is the loss of alkene observed only for La^+, which is a consequence of its two-valence electronic structure as first observed for Sc^+.[23] One additional result from this study is that the second ionization potential of LaC_2H_2 is about 11 eV (Table IV). Surprisingly, it is close to that of lanthanum (11.06 eV), which is in contrast to the case of $NbCH_2^{2+}$ where it was found that upon the addition of the carbene, the second ionization potential was lowered from 14.3 to 12 ± 1 eV.[16] The combination of experiment and theory will continue to shed light on these interesting systems.

Acknowledgment is made to the Division of Chemical Sciences in the Office of Basic Energy Sciences in the United States Department of Energy (DE-FG02-87ER13766) for supporting this research and to the National Science Foundation (CHE-8920085) for providing funds for the advancement of FTMS methodology. Y.A.R. would also like to thank Anne Gull for carrying out a gas chromatographic analysis on the ethane sample to quantitate ethylene impurity and also Dr. Yongqing Huang for his suggestions. The authors also thank Dr. Bauschlicher for his helpful discussions and the reviewers for their helpful comments.

Registry No. La^{2+}, 17643-88-8; $LaC_2H_4^{+}$, 128058-65-1; $LaC_2H_4^{2+}$, 128026-71-1; $LaC_3H_6^{+}$, 128026-67-5; $LaC_3H_6^{2+}$, 128026-73-3; $LaC_2H_2^{+}$, 128086-44-2; $LaC_2H_2^{2+}$, 128026-72-2; methane, 74-82-8; ethane, 74-84-0; propane, 74-98-6; butane, 106-97-8.

(26) Bauschlicher, C. W., Jr.; Langhoff, S. R.; Partridge, H. *J. Phys. Chem.* **1991**, *95*, 6191.
(27) Sodupe, M.; Bauschlicher, C. W., Jr.; Langhoff, S. R.; Partridge, H. *J. Phys. Chem.* **1992**, *96*, 2118.
(28) The heats of formation for C_3H_2 are the scaled ab initio value for propadienlidine (129 ± 4 kcal/mol) and propargylene (136 ± 4 kcal/mol) from: Clauberg, H.; Minsek, D. W.; Chen, P. *J. Am. Chem. Soc.* **1992**, *114*, 99.

Atmospheric Chemistry of Titan: Ab Initio Study of the Reaction between Nitrogen Atoms and Methyl Radicals

Carlos Gonzalez† and H. B. Schlegel*

Contribution from the Department of Chemistry, Wayne State University, Detroit, Michigan 48202. *Received September 23, 1991*

Abstract: Ab initio calculations were performed on the reaction N + CH_3 → products. Optimized geometries have been calculated for all reactants, transition states, and products at the MP2/6-31G** level. Barriers and heats of reaction have been estimated by fourth-order Møller–Plesset perturbation theory with spin projection (PMP4(SDTQ)). Harmonic vibrational frequencies and zero-point energy corrections were calculated at the MP2/6-31G** level. The two-step process $N(^4S)$ + CH_3 → $^3[CH_3N]$ → H_2CN + H appears to be the most important channel in this reaction.

Introduction

For the past 20 years, considerable research has been devoted to the atmospheres of Jupiter and its satellite Titan.[1] Early ground-based observations[1] indicate a large $[CH_4]/[H_2]$ ratio, which suggests that complex organic molecules could be formed via photochemical reactions. More recently, the Voyager missions have provided evidence that N_2 is the principal constituent of Titan's atmosphere,[1] followed by CH_4, H_2, C_2H_2, C_2H_4, C_2H_6, CH_3C_2H, C_3H_8, C_4H_2, HCN, HC_3N, C_2N_2, CH_2O, CO, CO_2, and H_2O. Consequently, in order to understand the dynamics of Titan's atmosphere, it is necessary to include reactions between nitrogen-containing species and hydrocarbons. The interaction of nitrogen atoms and methyl radicals is thought to be a significant path in the formation of HCN. Experimental rate constants obtained at room temperature by Stief et al.[2] and by Armstrong

* Author to whom correspondence should be addressed.
† Current address: Pittsburgh Supercomputing Center, Mellon Institute Building, Pittsburgh, PA 15213.

(1) Yung, Y. L.; Allen, M.; Pinto, J. P. *Astrophys. J. Suppl. Ser.* **1984**, *55*, 465.

0002-7863/92/1514-9118$03.00/0

Table I. Vibrational Frequencies for Minima and Transition Structures for the Reaction $N + CH_3 \rightarrow$ Products[a,b]

molecule	frequency (cm^{-1})
	Minima
CH_3	395 (424), 1491 (1381), 1491 (1383), 3244 (3184), 3442 (3002), 3442 (3002)
$^1[NCH_3]$	589 i, 962, 1099, 1446, 1481, 1500, 2237, 3064, 3170
$^3[NCH_3]$	1007, 1007, 1081, 1452, 1511, 1511, 3086, 3185, 3185
H_2CN	978, 1175, 1461, 2086, 3125, 3202
$^1[H_2CNH]$	1107, 1121, 1210, 1405, 1528, 1714, 3103, 3222, 3470
HCN	736 (727), 736 (727), 2045 (2129), 3537 (3441)
H_2	4611 (4401)
^3NH	3411
	Transition Structures
$^1[NCH\cdots H_2]$	1339 i, 428, 1067, 1283, 1479, 1743, 2420, 2566, 3103
$^3[NCH_2\cdots H]$	1053 i, 468, 644, 990, 1105, 1428, 1625, 3141, 3236
$^2[NCH\cdots H]$	1772 i, 667, 946, 1125, 2501, 3521
$^1[NCH\cdots H\cdots H]$	1262 i, 344, 440, 959, 1165, 1358, 1801, 2182, 3207
$^2[NCH\cdots H\cdots N]$	2465 i, 212, 461, 519, 917, 1102, 1349, 2258, 3254

[a] Frequencies calculated at the MP2(full)/6-31G** level. [b] Experimental frequencies in parentheses (ref 19).

and Winkler[3] seem to support this conclusion. In addition, Glarborg and co-workers[4] have suggested the importance of this reaction in the formation of nitrogen oxide species, as a result of a variety of combustion processes. The reaction between nitrogen atoms and methyl radicals is also considered to be a very important step in processes involving the cracking of hydrocarbons by active nitrogen.[5-7]

Recently, considerable effort has been focused on experimental studies leading to the elucidation of the possible mechanisms involved in the reaction $N + CH_3 \rightarrow$ products.[8-10] This reaction can proceed via the following thermodynamically active channels:

$$^2N + CH_3 \rightarrow HCN + H_2 \quad (1)$$

$$^4N + CH_3 \rightarrow H_2CN + H \quad (2)$$

$$^4N + CH_3 \rightarrow HCN + 2H \quad (3)$$

On the basis of a study of CH_4 reacting with mixtures of N and H atoms, Safrany[6] has proposed reaction 2 as the more important channel. Marston et al.[8] have measured the rate constant for $N + CH_3$ in the temperature range 200–423 K using discharge flow mass spectrometric techniques. The results show an unusual non-Arrhenius temperature dependence of the kinetics of this reaction. The best fit obtained by the authors gives the following rate expression:

$$k(T) = k_a + A_b \exp(-E_b/RT) \quad (4)$$

with $k_a = 3.7 \times 10^7$ cm^3 mol^{-1} s^{-1}, $A_b = 1.32 \times 10^{15}$ cm^3 mol^{-1} s^{-1}, and $E_b/R = 1250$ K. Equation 4 suggests the possibility of a two-channel mechanism, where one of them is temperature independent. However, as the authors explain, the value of A_b is too large, making this interpretation of eq 4 questionable. In an effort to understand the mechanism leading to such unusual behavior, Marston et al.[9] have measured the branching ratios of channels 1–3 by discharge flow techniques combined with mass spectrometry and concluded that about 90% of the reaction is dominated by channel 2, while approximately 10% of the reaction gives HCN + H. Even though these findings agree with the mechanism proposed by Safrany,[6] they contradict the common belief that suggests reaction 3 as the most important channel.[11] In addition, the lack of temperature dependence observed in the branching ratios[9] cannot explain the non-Arrhenius behavior of $CH_3 + N$.

In the present work, ab initio molecular orbital calculations are used in order to determine the energetics and possible mechanisms involved in the reaction $N + CH_3$.

Method

Ab initio molecular orbital calculations were performed with the GAUSSIAN system of programs.[12] Geometries were fully optimized at the Hartree–Fock and MP2 levels of theory with analytical gradients[13] using the 6-31G** basis set.[14] Harmonic vibrational frequencies and zero-point energies of the reactants, transition states, intermediates, and products were computed at second-order Møller–Plesset perturbation theory level using analytical second derivatives. Electron correlation was calculated with fourth-order Møller–Plesset perturbation theory in the space of single, double, triple, and quadruple excitations (MP4SDTQ, frozen core). Past studies have shown that the position of the barrier as well as the barrier height calculated at the UHF level is affected by a considerable amount of spin contamination of the transition states.[15-17] When spin contamination becomes significant, the barrier heights can be overestimated by up to 10 kcal/mol, even after correlation corrections calculated by Møller–Plesset perturbation theory are included.[18] In order to remove the spin contamination from higher spin states, an approximate spin projection method[15-17] was applied to the UHF wave function, and the corrected MP4 energies were computed (denoted here by PMP4).

Results

Figures 1 and 2 show the optimized geometries for the various stationary points for reactions 1–3, while the harmonic frequencies are listed in Table I. At the MP2/6-31G** level, the calculated frequencies are typically ca. 6% too high compared with experimental anharmonic frequencies because of basis set effects and neglect of anharmonicity. Table II shows the total energies at the MP2, MP4, and PMP4 levels calculated with the 6-31G** basis set at the MP2/6-31G** optimized geometry as well as the

(2) Stief, L. J.; Marston, G.; Nava, D. F.; Payne, W. A.; Nesbitt, F. L. *Chem. Phys. Lett.* **1988**, *147*, 570.
(3) Armstrong, D. A.; Winkler, C. A. *Can. J. Chem.* **1955**, *33*, 1649.
(4) Glarborg, P.; Miller, J. A.; Kee, R. J. *Combust. Flame* **1986**, *65*, 177.
(5) Titani, Y.; Lichtin, N. N. *J. Phys. Chem.* **1968**, *72*, 526.
(6) Safrany, D. R. *Prog. React. Kinet.* **1971**, *6*, 1.
(7) Michael, J. V. *Chem. Phys. Lett.* **1980**, *76*, 129.
(8) Marston, G.; Nesbitt, F. L.; Nava, D. F.; Payne, W. A.; Stief, L. J. *J. Phys. Chem.* **1989**, *93*, 5769.
(9) Marston, G.; Nesbitt, F. L.; Stief, L. J. *J. Chem. Phys.* **1989**, *91*, 3483.
(10) Nesbitt, F. L.; Marston, G.; Stief, L. J. *J. Phys. Chem.* **1990**, *94*, 4946.
(11) (a) Evans, H. G.; Freeman, G. R.; Winhler, C. A. *Can. J. Chem.* **1956**, *34*, 1271. (b) Safrany, D. R.; Jaster, W. *J. Phys. Chem.* **1968**, *72*, 518. (c) Herron, J. T. *J. Phys. Chem.* **1965**, *69*, 2736.
(12) Frisch, M. J.; Trucks, G. W.; Head-Gordon, M.; Gill, P. M. W.; Wong, M. W.; Foresman, J. B.; Johnson, B. G.; Schlegel, H. B.; Robb, M. A.; Replogle, E. S.; Gomperts, R.; Andres, J. L.; Raghavachari, K.; Binkley, J. S.; Gonzalez, C.; Martin, R. L.; Fox, D. J.; Defrees, D. J.; Baker, J.; Stewart, J. J. P.; Pople, J. A. GAUSSIAN 92; Gaussian, Inc.: Pittsburgh, PA, 1992.
(13) Schlegel, H. B. *J. Comput. Chem.* **1982**, *3*, 214.
(14) Hariharan, P. C.; Pople, J. A. *Chem. Phys. Lett.* **1972**, *66*, 217.
(15) Sosa, C.; Schlegel, H. B. *Int. J. Quantum Chem.* **1986**, *29*, 1001; *30*, 155.
(16) Sosa, C.; Schlegel, H. B. *Int. J. Quantum Chem., Quantum Chem. Symp.* **1987**, *21*, 267.
(17) Sosa, C.; Schlegel, H. B. *J. Am. Chem. Soc.* **1987**, *109*, 4193.
(18) Gonzalez, C.; Sosa, C.; Schlegel, H. B. *J. Phys. Chem.* **1989**, *93*, 2435, 8388.
(19) *JANAF Thermochemical Tables*, 2nd ed.; Natl. Stand. Ref. Data Ser. (U.S., Natl. Bur. Stand.) 37; U.S. GPO: Washington, DC, 1970.

Table II. Total Energies, Zero-Point Energies, and Entropies for the Reaction N + CH_3 → Products

species	total energy (au)[a] MP2	MP4	PMP4	ZPE (kcal/mol)[b]	entropy[b,c]	$\langle \hat{S}^2 \rangle$[d]
^4N	−54.457 008	−54.473 256	−54.473 597	0.00	36.60	3.7551
^2N	−54.390 764	−54.410 816	−54.378 505	0.00	35.23	1.7611
CH_3	−39.697 533	−39.714 734	−39.715 867	19.31	46.83	0.7612
$^1[NCH_3]$	−94.224 354	−94.263 618	−94.235 860	21.38	54.75	1.0095
$^3[NCH_3]$	−94.266 088	−94.292 544	−94.294 137	24.33	57.03	2.0191
$^1[NCH\cdots H_2]$ (ts)	−94.171 265	−94.201 406	−94.195 463	20.14	55.22	0.8769
$^3[H_2CN\cdots H]$ (ts)	−94.182 527	−94.211 380	−94.222 063	18.06	58.27	2.2672
$^2[HCN\cdots H]$ (ts)	−93.635 869	−93.659 824	−93.670 816	12.52	55.47	0.9532
$^1[CNH\cdots H\cdots H]$ (ts)	−94.186 243	−94.214 511	−94.240 247	16.38	57.21	1.0818
$^3[CNH\cdots H\cdots N]$ (ts)	−148.130 957	−148.173 083	−148.189 524	14.40	65.51	3.0027
H_2CN	−93.694 241	−93.721 057	−93.729 111	17.20	53.38	0.9071
$^1[H_2CNH]$	−94.349 286	−94.372 484	−94.372 484	25.56	54.26	0.0000
^3NH	−55.070 723	−55.087 348	−55.088 579	4.88	43.22	2.0137
HCN	−93.174 366	−93.188 306	−93.188 306	10.09	48.23	0.0000
H_2	−1.157 661	−1.164 560	−1.164 560	6.59	31.08	0.0000
H	−0.498 233	−0.498 233	−0.498 233	0.00	27.37	0.7500

[a] Calculated at the MP*n*(fc)/6-31G**//MP2(full)/6-31G** level. [b] Calculated at the MP2(full)/6-31G** level. [c] Entropy in cal/K mol, calculated at 298 K, 1 atm, ideal gas. [d] $\langle S^2 \rangle$ at the HF/6-31G**//MP2/6-31G** level.

Table III. Relative Energies[a] and Heats of Reaction[b] for the Reaction N + CH_3 → Products

species	ΔE_{MP2}	ΔE_{MP4}	ΔE_{PMP4}	ΔZPE	$\Delta H°_{298}$
$^4N + CH_3$	0.00	0.00	0.00	0.00	0.00
$^2N + CH_3$	41.57	39.18	59.67	0.00	59.67
$^1[NCH_3]$	−41.74	−45.39	−27.04	2.07	−28.66
$^1[NCH\cdots H_2]$ (TS)	−9.66	−7.59	−2.93	0.83	−4.95
$HCN + H_2$	−114.00	−106.09	−105.17	−2.63	−103.75
$^1[H_2CNH]$	−115.95	−109.52	−108.60	6.25	−110.23
$^3[NCH_3]$	−64.98	−60.59	−60.66	5.02	−62.26
$^3[H_2CN\cdots H]$ (TS)	−18.81	−15.93	−21.71	−1.25	−23.10
$^3[H_2CN + H]$	−25.91	−21.75	−25.88	−2.11	−26.05
$^3[HCN\cdots H + H]$ (TS)	6.04	11.99	6.02	6.79	5.94
HCN + 2H	−19.44	−7.20	−6.28	−9.22	−5.18
$^1[HCN\cdots H\cdots H]$ (TS)	−22.82	−19.57	−34.80	−2.93	−36.04
$^3[CNH\cdots H\cdots N]$ (TS)	−15.98	−11.23	−20.41	−4.91	−21.41
$^3NH + HCN$	−87.03	−75.02	−74.66	−4.34	−74.45

[a] Relative energies and ΔZPE in kcal/mol, calculated with respect to $^4N + CH_3$. [b] $\Delta H°_{298}$ includes ΔZPE and thermal corrections calculated at 298 K, 1 atm, ideal gas.

zero-point energy corrections (ZPE), entropies, and $\langle \hat{S}^2 \rangle$ for all the species involved in the reaction N + CH_3 → products. The corresponding relative energies and barrier heights are listed in Table III and shown schematically in Figure 3. At the PMP4/6-31G** level, the errors in the relative energies for non-isodesmic reactions can be as large as ±10 kcal/mol.

$^2N + CH_3 \rightarrow {}^1CH_3N \rightarrow HCN + H_2$, H_2CNH. The reaction on the singlet surface proceeds via singlet methylnitrene, $^1[CH_3N]$, which is 88 kcal/mol more stable than $^2N + CH_3$ and 29 kcal/mol more stable than $^4N + CH_3$. This is not a long range van der Waals complex; as shown in Figure 1a, the MP2 optimized structure has a tetrahedral carbon and a C–N bond 0.05 Å shorter than the C–N bond in CH_3NH_2. Unimolecular decomposition of this intermediate can occur by two pathways. Decomposition into HCN + H_2 has a barrier of 24 kcal/mol and is exothermic by 75 kcal/mol (see Figure 3). The structure of the transition state is shown in Figure 1b. On the basis of the C–H and H–H distances, it is more reactant-like, in agreement with Hammond's postulate; however, the C–N bond is closer to midway between reactants and products. The second path for decomposition involves a 1,2 hydrogen shift to form H_2CNH with an exothermicity of 82 kcal/mol (Figure 3). Singlet CH_3N has no imaginary frequencies at the HF level and, hence, has at least a small barrier for the 1,2 shift. The imaginary frequency found at the UMP2 level is a consequence of the SCF instability with respect to the lower lying triplet. Hartree–Fock studies of Pople et al.[20] and two-determinant wave-function calculations of Demuynck, Fox, Yamaguchi, and Schaefer[21] indicate there is no barrier for the

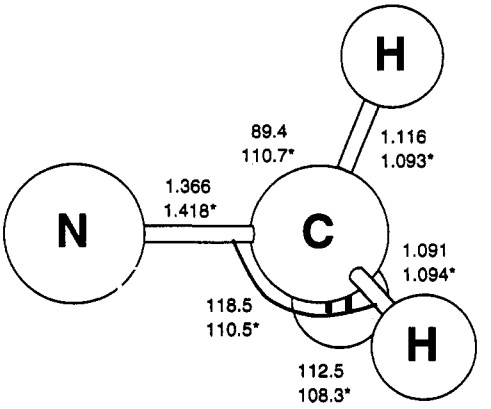

(a)

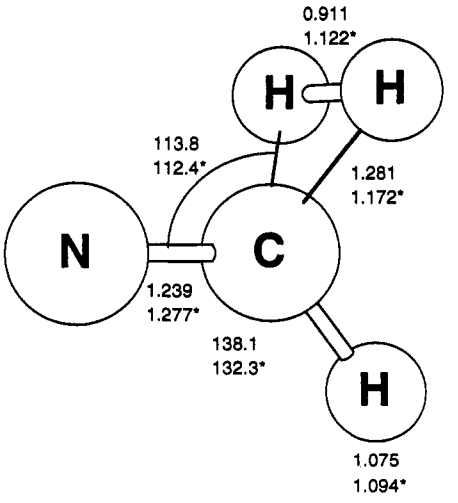

(b)

Figure 1. Intermediate (a) and transition state (b) for the reaction $^2N + CH_3 \rightarrow {}^1[CH_3N] \rightarrow HCN + H_2$ on the singlet energy surface, optimized at the HF/6-31G** level (no superscript) and the UMP2-(full)/6-31G** level (asterisk) (bond lengths in Å, angles in deg).

1,2 hydrogen shift, $^1[CH_3N] \rightarrow H_2CNH$.

$^4N + CH_3 \rightarrow {}^3CH_3N \rightarrow H_2CN + H$, $^4N \rightarrow HCN + 2H$, ^2NH. The reaction on the triplet surface occurs via a stable intermediate,

(20) Pople, J. A.; Raghavachari, K.; Frisch, M. J.; Binkley, J. S.; Schleyer, P.v.R. *J. Am. Chem. Soc.* **1983**, *105*, 6389.

(21) Demuynck, J.; Fox, D. J.; Yamguchi, Y.; Schaefer, H. F., III. *J. Am. Chem. Soc.* **1980**, *102*, 6204.

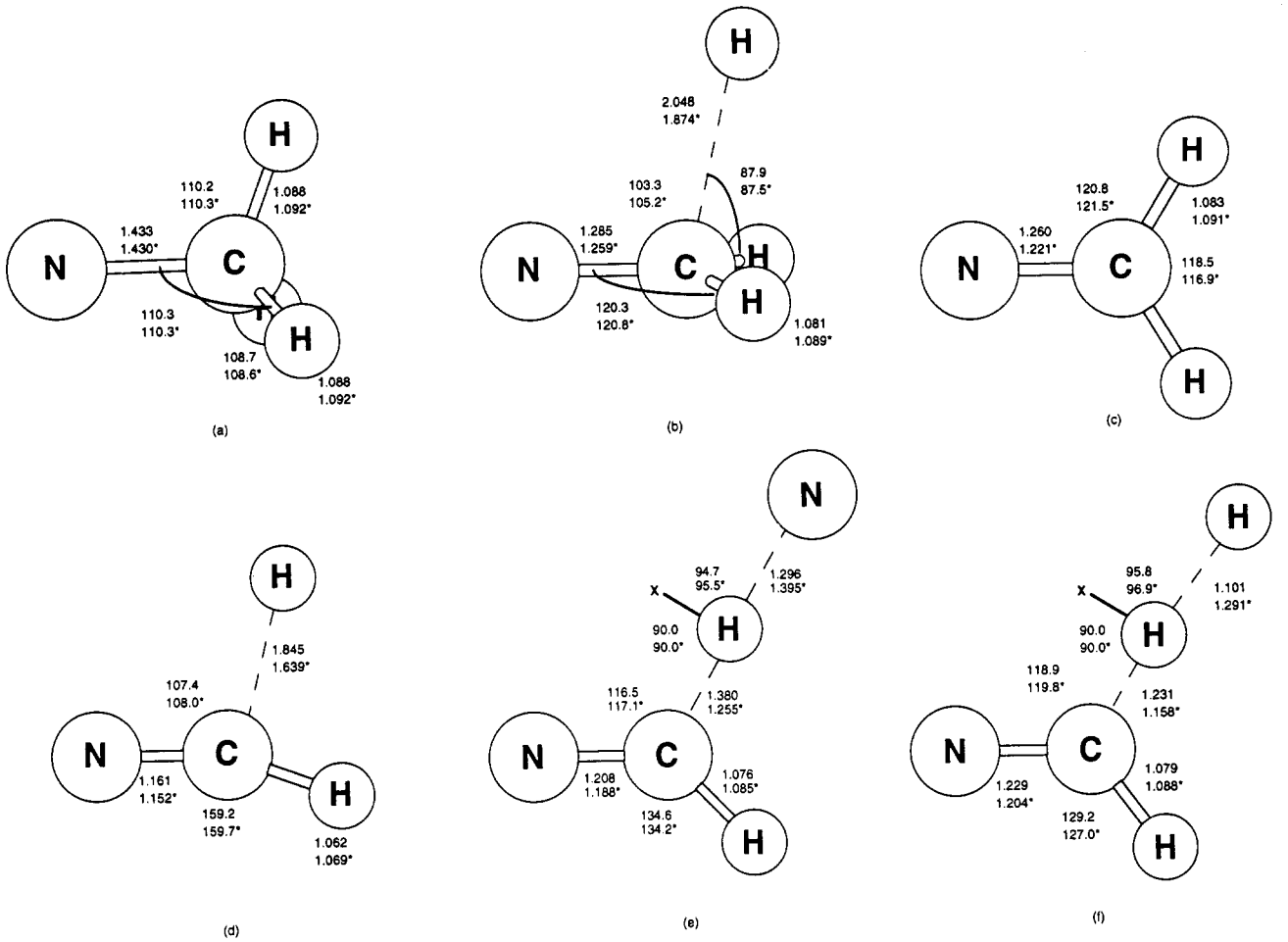

Figure 2. Intermediates and transition states for the reaction $^4N + CH_3 \rightarrow {}^3[CH_3N] \rightarrow H_2CN + H \rightarrow HCN + 2H$ on the triplet energy surface, optimized at the HF/6-31G** level (no superscript) and the UMP2(full)/6-31G** level (asterisk) (bond lengths in Å, angles in deg).

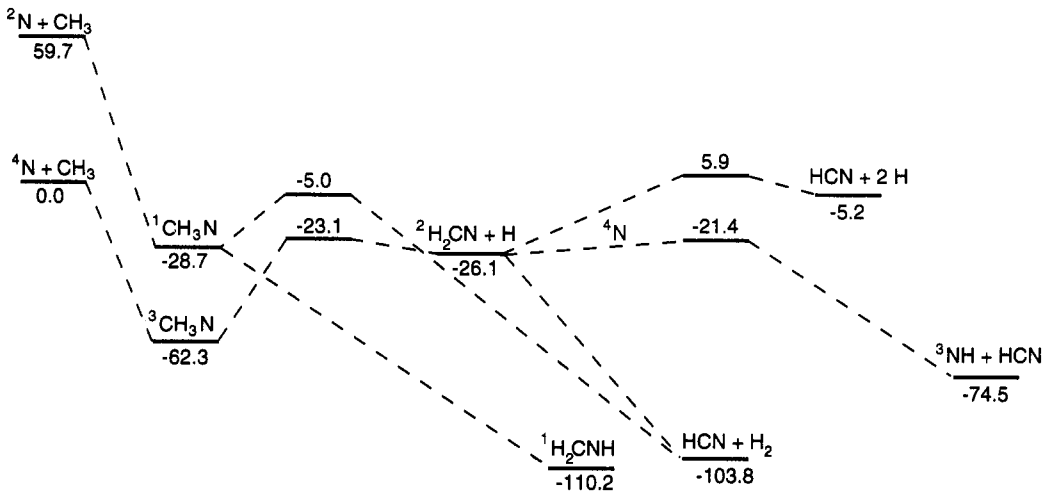

Figure 3. Calculated relative energies and barrier heights for the reaction N + CH_3 on the singlet and triplet surfaces ($\Delta H°_{298}$ in kcal/mol).

triplet methylnitrene, $^3[CH_3N]$, which is 62 kcal/mol more stable than $^4N + CH_3$. The triplet intermediate (Figure 2a) is structurally very similar to the singlet (Figure 1a) but ca. 34 kcal/mol more stable. The lowest energy pathway for unimolecular decomposition proceeds by loss of an H atom to yield H_2CN with a barrier of 39 kcal/mol (see Figure 3). This is an endothermic process (ΔH_r = 36 kcal/mol), and the transition state, Figure 2b, is more product-like. This transition state closely resembles those for other H additions to multiple bonds,[15,16,22] such as H + H_2CCH_2, HCCH, and CH_2O (i.e., long C–H with relatively little pyramidalization at carbon). Alternatively, H_2CN could be formed by a bimolecular reaction of $^3[CH_3N]$ with ^2H or ^4N; these reactions have not been explored in the present paper.

The intermediate H_2CN (Figure 2c) can undergo further unimolecular decomposition. Loss of a second hydrogen from H_2CN proceeds via a late transition state, Figure 2d, with a barrier of 32 kcal/mol, in good agreement with 30 kcal/mol obtained by Bair and Dunning[23] in a GVB-CI treatment of the H + HCN system. By analogy to the singlet surface, one might consider other pathways for decomposition of $^3[CH_3N]$ that include loss of H_2

(22) Sosa, C.; Schlegel, H. B. *J. Am. Chem. Soc.* **1987**, *109*, 7007.

(23) Bair, R. A.; Dunning, T. H., Jr. *J. Chem. Phys.* **1985**, *82*, 2280.

or 1,2 hydrogen migration; however, these are higher energy channels that lead to excited-state products.

The H_2CN intermediate can also participate in bimolecular reactions. Recombination with H and CH_3 are expected to be barrierless. Abstraction of a hydrogen from H_2CN by ^4N has a barrier of 4.7 kcal/mol, while hydrogen abstraction by H was found to have no barrier. Transition-state optimized geometries for the above processes are shown in parts e and f, respectively, of Figure 2. Abstractions by other radicals can be expected to be similar.

Discussion

The overall energetics for the reaction $N + CH_3 \rightarrow$ products are summarized in Figure 3. Among the three possible channels, reaction 2 on the triplet surface seems to be the most important pathway. Reaction 1 requires an excitation of ^4N to ^2N or an intersystem crossing to the singlet surface during the interaction of N and CH_3. Even though reaction 1 is considerably more exothermic (-104 kcal/mol vs -26. kcal/mol), the net reaction barrier on the singlet surface via excitation of ^4N to ^2N is considerably higher than that for reaction 2 on the triplet surface (-5 kcal/mol vs -23 kcal/mol).

Once the methyleneamino radical, H_2CN, is formed via reaction 2, it can undergo a unimolecular loss of hydrogen atom to give HCN; however, as shown in Figure 3, this process is endothermic with a significant barrier. Thus, reaction 3 as written can be ruled out as a possible channel in the reaction between N and CH_3. The hydrogen atom abstraction from H_2CN by H, ^4N, or CH_3 to give HCN is the more likely route for the disappearance of H_2CN.

The general features of the potential energy surface shown in Figure 3 provide some insight into the experimental findings of Marston et al.[8] It is apparent that the reaction proceeds on the triplet surface via the nitrene intermediate. Since all subsequent barriers are more than 20 kcal/mol lower than the energy of the reactants, $CH_3 + {}^4N$, it is unlikely that these barriers are rate determining at low temperatures.[24] Thus the formation of the triplet nitrene is most probably the rate-determining step. The temperature dependence of ion-molecule and radical recombination reactions has been studied in some detail.[25] Ion-molecule reactions have strong, long-range interactions that result in a negative temperature dependence. Radical recombinations, which are more closely related to $CH_3 + {}^4N$, have weaker, short-range interactions that can result in a positive temperature dependence. Thus an interpretation of the experimental rate expression for $CH_3 + {}^4N$, eq 4, will require a detailed study of the $CH_3 + {}^4N$ interaction potential and a proper theoretical treatment of the kinetics of the formation of $^3[CH_3N]$ and its subsequent decomposition. This is a topic for future research.

Conclusions

Ab initio calculations have been carried out to study the possible mechanisms involved in the reaction between ground-state nitrogen atoms and methyl radicals. Among the three possible processes considered, the reaction $N(^4S) + CH_3 \rightarrow {}^3[CH_3N] \rightarrow H_2CN + H \rightarrow HCN + H_2$ was found to be the most important pathway. The results of the present work provide theoretical evidence for the existence of a two-step mechanism that could shed new light on the non-Arrhenius behavior observed experimentally.[8]

Acknowledgment. We would like to thank Prof. W. L. Hase for numerous and helpful discussions. This work was supported by a grant from the National Science Foundation (CHE 90-20398) and by the Pittsburgh Supercomputing Center. Generous amounts of computer time from the computer center at Wayne State University are also gratefully acknowledged.

Registry No. $N(^4S)$, 17778-88-0; CH_3, 2229-07-4; CH_3N, 27770-42-9; H_2CN, 15845-29-1; HCN, 74-90-8.

(24) Steinfeld, J. I.; Francisco, J. S.; Hase, W. L. *Chemical Kinetics and Dynamics*; Prentice-Hall: Old Tappan, NJ, 1989.
(25) Hu, X.; Hase, W. L. *J. Phys. Chem.* **1989**, *93*, 6029 and references therein. Clary, D. C.; Werner, H.-J. *Chem. Phys. Lett.* **1984**, *112*, 346 and references therein.

Detection of Trace Species in Hostile Environments Using Degenerate Four-Wave Mixing: CH in an Atmospheric-Pressure Flame

Skip Williams, David S. Green, Srinivasan Sethuraman, and Richard N. Zare*

Contribution from the Department of Chemistry, Stanford University, Stanford, California 94305.
Received December 27, 1991. Revised Manuscript Received February 7, 1992

Abstract: Degenerate four-wave mixing (DFWM) has been used to detect the CH radical in an atmospheric-pressure oxyacetylene flame via the (0,0) and (1,1) bands of the $A^2\Delta$-$X^2\Pi$ transition. The reliability of DFWM has been assessed by comparing it to laser induced fluorescence (LIF) measurements under the same experimental conditions. The CH radical is a minor flame species (~30 ppm) and is important for understanding the primary reaction zone of many combustion environments. We have observed CH radicals with comparable sensitivity by both techniques. From these measurements, we estimate a DFWM detection limit of 4×10^{11} cm^{-3} [4×10^9 cm^{-3}/(quantum state)] for CH at atmospheric pressure. Vibrational temperatures and concentration profiles of CH obtained by both DFWM and LIF were in good agreement. The DFWM line-center signal intensities and line shapes were measured as a function laser intensity and were found to be consistent the model presented by Abrams and Lind. Based on these results, we suggest that DFWM can provide quantitative information regarding trace molecular species in high-pressure, high-temperature environments in which source emission hinders analysis by other means.

I. Introduction

Highly luminous sources, such as arcs, sparks, flames, explosions, plasmas, and discharges, pose a severe challenge to those who wish to probe their chemical composition, kinetics, and dynamics as a function of spatial distribution and temporal evolution. Nonintrusive optical methods,[1] like laser induced fluorescence (LIF), are hindered by interference from background emission, distortions caused by source temperature and density inhomo-

* Author to whom correspondence should be addressed.

(1) Eckbreth, A. C. *Laser Diagnostics for Combustion Temperature and Species*; Abacus: Cambridge, MA, 1988; Chapters 1, 5-7.

0002-7863/92/1514-9122$03.00/0